

# Imaging and autocorrelation of ultrafast infrared laser pulses in the 3–11- $\mu\text{m}$ range with silicon CCD cameras and photodiodes

Kimberly A. Briggman, Lee J. Richter, and John C. Stephenson

National Institute of Standards and Technology, Gaithersburg, Maryland 20899

Received July 28, 2000

Standard silicon photodiodes and CCD cameras are convenient and inexpensive alternatives to cryogenically cooled diodes or arrays for autocorrelation and imaging of ultrafast IR laser pulses in the wavelength range 3–11  $\mu\text{m}$ . The response of these Si devices to IR pulses of duration  $\sim 100$  fs is proportional to  $E^n$ , where  $E$  is the pulse energy and  $n$  is approximately the Si electronic bandgap divided by the photon energy. © 2001 Optical Society of America

OCIS codes: 040.1520, 040.3060, 040.6040, 190.7110, 190.4720, 140.7090.

Femtosecond laser technology permits the production of tunable IR laser pulses over the wavelength range  $\lambda = 1.2\text{--}20$   $\mu\text{m}$  by phase-matched optical parametric generation and difference-frequency mixing in nonlinear crystals. These IR pulses are used in a variety of dynamic, spectroscopic, and imaging applications in physics, chemistry, and biology. Crucial to applications is the determination of the spatial profile and the duration of the pulses. Many pump–probe and nonlinear mixing experiments such as sum-frequency generation (SFG) require matching the spatial profile and timing of a visible laser pulse with an IR pulse in the 3–11- $\mu\text{m}$  region at the interface of interest.<sup>1</sup> We discovered that standard Si CCD arrays used to determine the spatial profiles of visible pulses also respond to short-duration IR pulses. This property has proved useful because the only devices known to image IR lasers in this  $\lambda$  range are microbolometers and cryogenically cooled HgCdTe diode arrays, which are harder to use, more expensive, and have less spatial resolution than standard CCD cameras. In this Letter we describe practical applications in which the nonlinear response of Si devices to IR light is used for laser beam profiling and pulse autocorrelation. The Letter is not a quantitative fundamental study of nonlinear multiphoton absorption in Si.

Inasmuch as the electronic bandgap in Si is  $\sim 1.12$  eV ( $\lambda \sim 1.1$   $\mu\text{m}$ , or  $\nu \sim 9034$   $\text{cm}^{-1}$ ) at room temperature,<sup>2</sup> it might seem surprising that a Si device would respond to light in the range  $\lambda = 3\text{--}11$   $\mu\text{m}$ , e.g., with the energy of 3–9 photons needed to create an electron–hole pair in bulk Si. Two-photon-induced photoconductivity in a Si CCD camera was used previously<sup>3</sup> to image light at  $\lambda = 1.41$   $\mu\text{m}$ . Likewise, temporal autocorrelation<sup>4–8</sup> and cross correlation<sup>9</sup> of near-IR ultrafast laser pulses by an approach similar to that described here was reported for  $h\nu_1$ ,  $h\nu_2 < E_{\text{gap}} < (h\nu_1 + h\nu_2)$ . For these two-photon processes, signal  $S$  scales as the square of the laser intensity  $I(\nu)$ ,  $S \sim I(\nu)^2$  or  $S \sim I(\nu_1) \times I(\nu_2)$ , as for traditional frequency doubling or summing in phase-matched nonlinear crystals ( $n = 2$  scaling). Recently, three-photon autocorrelation of near-IR pulses in GaAsP (Ref. 10) and GaN (Ref. 11) photodiodes was reported. We are unaware of any previous

reports of the use of higher-order processes for laser beam imaging or autocorrelation–cross correlation at the long  $\lambda$  reported here, which are important for chemical applications of lasers.

We measured the response of several Si detectors as a function of laser pulse energy at several IR  $\lambda$ . The IR pulses are generated by a standard system in which a Ti:sapphire laser, amplified at 1 kHz, produces 800-nm pulses that pump an optical parametric amplifier generating signal ( $\lambda = 1.1\text{--}1.6$   $\mu\text{m}$ ) and idler ( $\lambda = 1.6\text{--}2.9$   $\mu\text{m}$ ) pulses. Tunable IR radiation in the region  $\lambda = 2.5\text{--}11$   $\mu\text{m}$  is generated in a AgGaS<sub>2</sub> crystal as the difference frequency between signal and idler pulses. The linearly polarized IR beam was attenuated by a wire grid polarizer rotated to give the desired IR energy and was focused onto the diode or CCD chip at normal incidence with a 10-cm focal-length BaF<sub>2</sub> lens. The pulse energy was measured with a pyroelectric detector (Laser Probe RjP-445 with an RM-3700 reader<sup>12</sup>; 5% accuracy claimed by the vendor for  $\lambda$  of 0.8–11  $\mu\text{m}$ ). The diode (or CCD) was mounted such that the diode–lens distance could be scanned. In Fig. 1 is shown the IR response of a common Si P–I–N photodiode

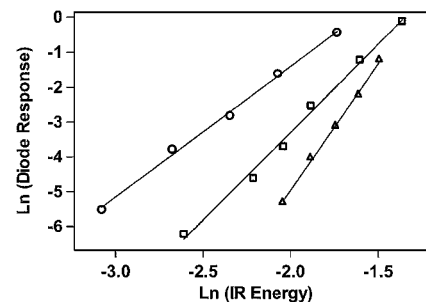


Fig. 1. Voltage response of a Si photodiode to IR laser pulses plotted as a function of pulse energy for IR  $\lambda$  of 3.45 (circles), 4.95 (squares), and 7.87 (triangles)  $\mu\text{m}$ . The signal (into 50  $\Omega$ ) is in volts and the energy is in microjoules. The response for  $\lambda = 3.45$   $\mu\text{m}$  has a slope  $n = 3.7 \pm 0.2$ ; for  $\lambda = 4.95$  and 7.87  $\mu\text{m}$  the slopes are  $5.0 \pm 0.4$  and  $7.2 \pm 0.4$ , respectively. The pulse duration is  $\sim 0.13$  ps; beam areas (50% energy) at the focus are  $\sim 4.5 \times 10^{-5}$ ,  $6.5 \times 10^{-5}$ , and  $8 \times 10^{-5}$   $\text{cm}^2$  for the 3.45-, 4.95-, and 7.87- $\mu\text{m}$  beams, respectively.

(Hamamatsu diode S-1223-01/Thor Labs Model DET2-Si; biased at 22 V, unamplified, 1-mm<sup>2</sup> active area, 1-ns response time)<sup>12</sup>; the voltage output into 50  $\Omega$  was recorded on an oscilloscope versus the pulse energy,  $E$ . The glass window was removed from the Si diode for these measurements, as glass does not transmit IR radiation at the longer wavelengths. For an IR  $\lambda = 3.45 \mu\text{m}$ , the data are fitted by a straight line of slope  $3.7 \pm 0.2$ ,<sup>13</sup> i.e., signal  $\sim E^n$ , with  $n = 3.7$ . Similar straight lines are displayed for  $\lambda = 4.95$  and  $\lambda = 7.87 \mu\text{m}$ , for which the power-law values of  $n$  are  $5.0 \pm 0.4$ , and  $7.2 \pm 0.4$ , respectively. The ratio of the Si bandgap to the photon energy at these three frequencies is 3.12, 4.47, and 7.11, respectively. Noninteger slopes are to be expected with IR pulses of such spectral width 200–400  $\text{cm}^{-1}$ ;  $\Delta\lambda/\lambda \sim 0.14$ ). For instance, for  $\lambda \sim 3.45 \mu\text{m}$ , blue-edge photons can create  $e^-h$  pairs by simultaneous multiphoton absorption of three photons, whereas red-edge photons would require a four-photon process (presumably all energy-conserving convolutions occur). The observed value of  $n = 3.7 \pm 0.2$  is consistent with multiphoton absorption of several IR quanta, creating an  $e^-h$  pair, although our data do not prove that this is the mechanism for the photocurrent. Similar responses were seen for other Si photodiodes. At sufficiently high IR energies, the response saturated; i.e., the voltage waveform became distorted and the response fell below the lines shown in Fig. 1. A highly nonlinear response,  $n > 7$ , was also seen for IR at  $\lambda = 11 \mu\text{m}$ , although laser pulse instability and extreme nonlinearity made determination of  $n$  difficult at that  $\lambda$ . We suspect that other diodes (Ge, InGaAs, GaAsP, etc.), which have different effective  $E_{\text{gap}}$  values, would show similar scaling of  $n \sim E_{\text{gap}}/\text{photon energy}$ .

A similar nonlinear response to IR light occurs for standard Si CCD video cameras used for laser beam spatial profiling. Figure 2 shows the response of a CCD camera (Pulnix Model TM-7CN; 9- $\mu\text{m}$  pixel size, windowless, signal digitization resolution of  $2^8$ ) to light at 3.45  $\mu\text{m}$ . At a point 23 mm before the focus of the lens, the image is oval, with apparent dimensions of 220  $\mu\text{m}$  by 340  $\mu\text{m}$  FWHM. The IR beam is larger in the vertical than in the horizontal dimension because of phase matching in the AgGaS<sub>2</sub> crystal used to generate the IR; i.e., the different frequencies of the 400  $\text{cm}^{-1}$  broad IR beam are slightly dispersed in the vertical dimension. The IR laser pulse energy incident upon the CCD chip was 2.9  $\mu\text{J}$  for this image. Similar images were recorded at this  $\lambda$  with another camera (Cohu Model 4800; 25- $\mu\text{m}$  pixel size, silica window). For the latter camera, the response integrated over the chip to light at this  $\lambda$  scaled the same with IR energy, within experimental uncertainty, as for the simple photodiode, e.g.,  $n = 3.5 \pm 0.3$ . To convert the recorded image into the true spatial profile, presumably one should take the response of each pixel and raise it to the  $1/n$ th power, where  $n$  is the experimentally determined response for the pulses that are being imaged. If the beam can be approximated as a Gaussian,  $I = I_{\text{max}} \exp(-2r^2/w^2)$ , then one should multiply beam waist  $w$  derived from the fit to the image by  $\sqrt[n]{1.9}$  to estimate the true

value of  $w$ , as would be recorded by a camera with a linear response. The technique is a useful alignment tool rather than a highly accurate pulse and beam characterization method. For precise work, a camera setup with digitization accuracy better than  $2^8$  should be used. Also, if spectrally broad beams had severe spatial chirp, e.g., if the top of the beam contained the bluest colors (lowest multiphoton order  $n$ ) and the bottom the reddest (lowest order  $n + 1$ ), quantitative interpretation might require additional measurements, such as a power-dependent study of the image size (in principle, determining  $n$  effective for each pixel). Despite such concerns, CCD cameras have been particularly useful to us in aligning the spatial overlap of the visible ( $\sim 800\text{-nm}$ ) beam with the IR beam in our SFG experiments. Images of the IR beam spatial profile were also recorded with the windowless CCD camera for IR light at  $\lambda$  of 4.95, 7.87, and 10  $\mu\text{m}$ .

The laser intensities in the experiments can be estimated as follows: The horizontal axis in Fig. 1 gives the IR pulse energy in microjoules; the lowest point for the 3.45- $\mu\text{m}$  line corresponds to an energy incident upon the diode of 0.04  $\mu\text{J}$  (much of which could be reflected from the first surface because of the high refractive index of Si or the overlying metalization). The IR spot size at the focus of the 10-cm focal-length BaF<sub>2</sub> lens at this  $\lambda$  was  $\sim 4.5 \times 10^{-5} \text{ cm}^2$  in area (50% included energy from a Gaussian fit to the CCD image at the focus), and the pulse duration (see below) was  $t_p \sim 0.13 \text{ ps}$ , corresponding to a fluence of  $\sim 10^{-3} \text{ J/cm}^2$  or a peak incident intensity of  $I \sim 10^{10} \text{ W/cm}^2$ . For both the Cohu and the Pulnix CCD setups, a full-intensity ( $2^8$ ) image was obtained at a reasonable amplifier gain for an incident fluence of  $\sim 0.001 \text{ J/cm}^2$ , for light at  $\lambda = 3.45 \mu\text{m}$ ; the required fluence ( $\text{J/cm}^2$ ; Pulnix) to produce the same signal at 10  $\mu\text{m}$  was  $\sim 2.8$  times greater than for 3.45  $\mu\text{m}$ . For the Pulnix chip at the focus of the lens, the 3.45- $\mu\text{m}$  pulses caused slight pixel damage within 5 s at an energy of 1.6- $\mu\text{J}$ /pulse (1-kHz repetition rate onto the chip,  $t_p \sim 0.13 \text{ ps}$ , fluence/pulse,  $\sim 0.04 \text{ J/cm}^2$ ); a pulse energy of 1.0  $\mu\text{J}$  did not cause pixel damage, at least over a 10-s time interval.

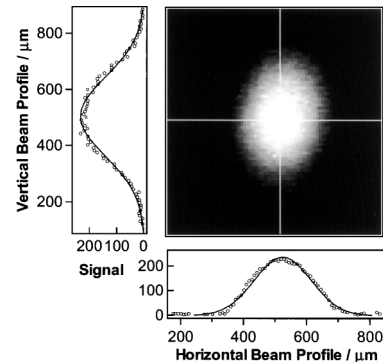


Fig. 2. Spatial profile of an IR laser pulse at  $\lambda = 3.45 \mu\text{m}$  recorded by a Si CCD camera with 9- $\mu\text{m}$  pixel spacing. Pulse duration,  $\sim 0.13 \text{ ps}$ ; energy,  $\sim 2.9 \mu\text{J}$ . The image has a FWHM of 220  $\mu\text{m}$  (horizontal) by 340  $\mu\text{m}$  (vertical). Because of the nonlinear response of Si at this wavelength, the true beam diameters are  $\sim 1.9$  times these values.

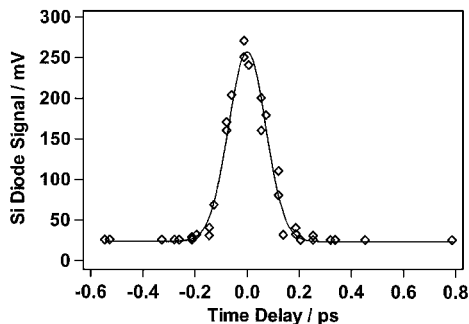


Fig. 3. Noncollinear autocorrelation trace for use in determining the duration of a laser pulse at  $\lambda = 3.45 \mu\text{m}$  by use of the nonlinearity of a Si photodiode to IR light at this wavelength (same diode and spot size as for the  $3.45\text{-}\mu\text{m}$  trace in Fig. 1; pulse energy scaling,  $n \sim 3.7$ ). The curve through the data points is a Gaussian fit with a FWHM of  $0.17 \pm 0.2$  ps, which, assuming balanced Gaussian pulses, implies a pulse duration of 0.15 ps. The ratio of peak to pedestal signal depends on the energy balance and spatial overlap of the beams.

One can easily use the nonlinear response to determine the pulse duration through autocorrelation or cross correlation. The duration of the amplified 800-nm pulses that we used to generate the IR pulses is measured by a conventional intensity autocorrelator, where each 800-nm pulse is split into two pulses; one is delayed with respect to the other, and the split pulses are noncollinearly combined and frequency doubled in a thin KDP crystal (a process scaling as  $I^2$ ). The 400-nm light is recorded as a function of delay between the pulses from the two arms of the interferometer. To determine the duration of the IR pulses by using the nonlinear response of Si, we sent the IR along the same path used for the 800-nm pulses. Where the KDP crystal had been previously positioned and where the noncollinear beams crossed, we placed a Si photodiode. A moving retroreflector changed the arrival time of one IR pulse with respect to the other; because of the strong nonlinearity in Si, when both IR pulses overlapped in the diode at the same time the diode output greatly increased. Figure 3 shows the autocorrelation of pulses of  $3.45\text{-}\mu\text{m}$  wavelength. The FWHM of the autocorrelation peak ( $0.17 \pm 0.02$  ps) is estimated by a fit to a Gaussian plus a constant. It is well known that, for pulses that are Gaussian in time, the FWHM of the autocorrelation trace is 1.414 times the FWHM of the pulse for the ordinary  $n = 2$  scaling seen for frequency doubling. The form of the non-background-free autocorrelation is not strictly Gaussian when  $n > 2$ . For  $n = 3.6$ , numerical simulation shows that the autocorrelation FWHM (for balanced Gaussian pulses) is 1.14 times the laser pulse duration. (This factor is 0.98 for  $n = 5$  and 0.80 for  $n = 7.3$ , corresponding to the wavelengths of 5.0 and  $7.9 \mu\text{m}$  mentioned above.) This implies that the IR laser pulses were  $0.15 \pm 0.02$  ps at the Si diode. For these higher-order autocorrelations there is a slight dependence of the FWHM on the relative

energy going into each arm or on the spatial overlap at the diode; e.g., for  $n = 3.6$ , an energy imbalance of a factor of 8 would increase the FWHM by  $\sim 9\%$ .

We used an independent method to measure the IR pulse duration. The compressed amplified 800-nm pulses were measured in the 800-nm autocorrelator to have a duration of 50 fs. These pulses were then mixed on a gold surface (SFG using the nonresonant  $\chi^2$  of gold) with the IR pulses, and the resultant SFG from 630 to 730 nm was recorded as a function of 800-nm IR time delay. This measurement gave an IR pulse duration of  $0.13 \pm 0.02$  ps, agreeing with the Si result within experimental uncertainty. As discussed above, if the pulses are temporally chirped, precise quantitative interpretation of the Si multiphoton autocorrelation would require additional experiments, assumptions (e.g., linear chirp), or modeling. However, agreement of the two autocorrelation methods for our pulses suggests that, at the limits of accuracy claimed here, autocorrelation in Si is easy and useful, obviating the need for cryogenic detectors and expensive thin nonlinear crystals for phase-matched doubling of these IR wavelengths.

Kimberly A. Briggman is a National Institute of Standards–National Research Council postdoctoral fellow. J. C. Stephenson's e-mail address is john.stephenson@nist.gov.

## References

1. L. J. Richter, T. P. Petrali-Mallow, and J. C. Stephenson, *Opt. Lett.* **23**, 1594 (1998).
2. W. Bludau, A. Onton, and W. Heinke, *J. Appl. Phys.* **45**, 1846 (1974).
3. Y. Takagi, T. Kobayashi, K. Yoshihara, and S. Imamura, *Opt. Lett.* **17**, 658 (1992).
4. W. Rudolph, M. Sheik-Bahae, A. Bernstein, and L. F. Lester, *Opt. Lett.* **22**, 313 (1997).
5. L. P. Barry, P. G. Bolland, J. M. Dudley, J. D. Harvey, and R. Leonhardt, *Electron. Lett.* **32**, 1922 (1996).
6. C. McGowan, D. T. Reid, M. Ebrahimzadeh, and W. Sibbett, *Opt. Commun.* **134**, 186 (1997).
7. A. Gutierrez, P. Dorn, J. Zeller, D. Kong, L. F. Lester, W. Rudolph, and M. Sheik-Bahae, *Opt. Lett.* **24**, 1175 (1999).
8. J. K. Ranka, A. L. Gaeta, A. Baltuska, M. S. Pshenichnikov, and D. A. Wiersma, *Opt. Lett.* **22**, 1344 (1997).
9. W. Schade, D. L. Osborne, J. Preusser, and S. R. Leone, *Opt. Commun.* **150**, 27 (1998).
10. P. Langlois and E. Ippen, *Opt. Lett.* **24**, 1868 (1999).
11. A. M. Streltsov, K. D. Moll, A. L. Gaeta, P. Kung, D. Walker, and M. Razeghi, *Appl. Phys. Lett.* **75**, 3778 (1999).
12. Certain commercial equipment, instruments, or materials are identified in this Letter to specify adequately the experimental procedure. In no case does such identification imply recommendation or endorsement by the National Institute of Standards and Technology, nor does it imply that the materials or equipment identified are necessarily the best available for the purpose.
13. All uncertainties are reported as twice the standard deviation,  $\sigma$ , obtained by least-squares fits.